Atmospheric Research 192 (2017) 30–37

Contents lists available at ScienceDirect

Atmospheric Research

journal homepage: www.elsevier.com/locate/atmosres

Contributions of Asian pollution and SST forcings on precipitation change in the North Pacific

Sang-Wook Yeh [a,*], Jihyeon So [a], Jong-Won Lee [a], Minjoong J. Kim [b], Jaein I. Jeong [b], Rokjin J. Park [b]

[a] Marine Sciences and Convergent Technology, Hanyang University, ERICA, Republic of Korea
[b] School of Earth and Environmental Sciences, Seoul National University, Republic of Korea

ARTICLE INFO

Article history:
Received 24 August 2016
Received in revised form 19 January 2017
Accepted 17 March 2017
Available online 18 March 2017

Keywords:
Pollutant aerosols
Particulate matter 2.5
GESO-Chem
Precipitation
North Pacific
El Nino-like warming

ABSTRACT

East Asia has a significant concentration of pollutant aerosols, mostly due to rapid industrialization. Previous research indicates that the aerosol effect from Asian pollution outflow could account for the trend of increasing deep convective clouds, as well as an intensification of the storm track, over the North Pacific Ocean in winter since the mid-1990s. However, it is not clear whether such change is solely due to Asian pollutant forcings or not. To understand the relative roles of Asian pollutant aerosols and sea surface temperature (SST) forcings on the precipitation change in the North Pacific, we examine the interannual variation of particulate matter 2.5 ($PM_{2.5}$) simulated in the global chemical transport model (GEOS-Chem) and the idealized experiments using the Community Atmosphere Model version 5 (CAM5) for 1986–2010. The composite analysis indicates that the changes in precipitation amount and storm track intensity in the southwestern North Pacific might be associated with the increase in $PM_{2.5}$ concentration in East China. However, El Niño-like warming during the years of high $PM_{2.5}$ concentration may also influence the precipitation amount, as well as the storm track intensity in the central and eastern North Pacific. Model experiments also indicate that the El Niño-like warming and the Asian pollutant aerosols have different effects on precipitation amounts in the North Pacific. Therefore, the precipitation changes, as well as the intensification of the storm track, in the North Pacific might be attributed to both Asian pollutant aerosols and SST forcing in the tropics.

1. Introduction

Pollutant aerosols, such as sulfate aerosols, black carbon, methane and tropospheric ozone, have relatively short atmospheric lives and are the most important contributors to radiative forcing in the climate system (Allen et al., 2016; Stocker et al., 2013). Most previous studies suggested that changes in the concentration of pollutant aerosols in the atmosphere can affect the variability of weather and climate through the modification of temperature and precipitation by altering cloud development or duration (Haywood and Boucher, 2000; Ackerman et al., 2000; Chung et al., 2002; Meehl et al., 2008; Lee et al., 2013; Jeong and Park, 2013; Kim et al., 2016). Specifically, pollutant aerosols alter the microphysical and optical properties of cloud droplets by acting as cloud condensation nuclei (CCN), which is known as the indirect effect. This indirect effect is divided into two different effects. The first effect is that the cloud droplet effective radius decreases as the concentration of pollutant aerosols increases, leading to an invigoration of convective clouds (Jiang and Feingold, 2006). On the other hand, the second indirect effect is that the decrease in the cloud droplet effective radius also results in an increase in cloud lifetime and an inhibition of precipitation (Albrecht, 1989).

In spite of numerous studies on the influence of pollutant aerosols, it is still uncertain how pollution particles affect precipitation variability (Albrecht, 1989; Stevens and Feingold, 2009; Tao et al., 2012). Furthermore, East Asia, including China, has experienced rapid economic development over the past three decades (Zhao et al., 2010), accompanied by increased emission of pollutant particles (Lu et al., 2011). This increase in East Asian pollution may impact climate variability in the North Pacific due to long-range transport of Asian pollutant particles (Yeh et al., 2013, 2015; Boo et al., 2015; Wang et al., 2014). By simulating a cloud-resolving weather research and forecast model, Zhang et al. (2007, hereafter, Z07) argue that the trend of increasing deep convective clouds over the North Pacific Ocean in winter since the mid-1990s could be explained by the aerosol effect from the Asian pollution outflow. That is, an increase in aerosol concentration over the North Pacific leads to large-scale enhanced convection and precipitation through an invigoration effect, and hence an intensified storm track over the Pacific (Z07). Through an invigoration effect, the high concentration of pollutant aerosols reduces the cloud droplet size for a fixed liquid water

* Corresponding author at: ERICA, Hanyang University, Republic of Korea.
E-mail address: swyeh@hanyang.ac.kr (S.-W. Yeh).

http://dx.doi.org/10.1016/j.atmosres.2017.03.014
0169-8095/

content (Twomey, 1974, 1977; Fan et al., 2009; Wang, 2013). Subsequently, the reduced cloud droplet size leads to more intensive thunderstorms and the release of more latent heat higher in the atmosphere (Zhou et al., 2008; You et al., 2011).

On the other hand, numerous studies indicate that the precipitation variability, as well as the intensity of the storm track, in the North Pacific is largely associated with variations in sea surface temperature (SST) in the tropical Pacific during the boreal winter, such as El Niño-Southern Oscillation (ENSO) (Lau and Nath, 1996, Chang et al., 2002 reference therein). Tropical Pacific SST fluctuations are able to produce a strong response in the North Pacific through atmospheric teleconnections, resulting in changes in precipitation amounts, as well as the storm track intensity. Therefore, both Asian pollution and tropical SST forcing should be considered to understand changes in precipitation amount and intensity in the North Pacific since the mid-1990s, which was not discussed in Z07.

In this study, we analyze the interannual variation of the particulate matter 2.5 ($PM_{2.5}$) concentration during the boreal winter (December to February) and its relationship with precipitation variability in the North Pacific for 1986–2010. The diameter of $PM_{2.5}$ is less than 2.5 μm. East Asia, including China, is an area with very high $PM_{2.5}$ concentrations (Elliott et al., 1997; Van Aardeen et al., 1998). $PM_{2.5}$ particles include sulfate, nitrate, ammonium, black carbon and organic carbon. For this study, $PM_{2.5}$ concentration was obtained from the global chemical transport model (GEOS-Chem) driven by meteorological input from the Modern Era-Retrospective Analysis for Research and Applications of the National Aeronautics and Space Administration (MERRA NASA) for 1985–2010 (Rienecker et al., 2011). We further examine the role of SST forcing in the tropics on the precipitation amount in the North Pacific by conducting idealized experiments using the NCAR Community Atmosphere Model version 5 (CAM5) model coupled with the Community Land Surface Model version 4 (Neale et al., 2010). Detailed explanations of the idealized experiments are provided in Section 2.

2. Data and methodology

2.1. GEOS-Chem simulation

We run the GEOS-Chem model to conduct a fully coupled oxidant-aerosol simulation (Park et al., 2004). The GEOS-Chem model v9–01-02 (http://acmg.seas.harvard.edu/geos/index.html) uses assimilated meteorology from MERRA NASA (Rienecker et al., 2011) including winds, convective mass fluxes, mixed layer depths, temperature, precipitation, and surface properties. The GEOS-Chem simulations have been applied to a number of air chemistry issues, including tropospheric aerosols, and have been extensively evaluated by comparison against observations in the U.S., Europe, and Asia. The Asian emissions of nitrogen oxides (NO_X), sulfur dioxide (SO_2), and ammonia (NH_3) are 9.1 Tg N y^{-1}, 18.9 Tg S y^{-1}, and 21.8 Tg N y^{-1}, respectively. We apply annual scale factors of Regional Emission inventory in Asia (REAS; Ohara et al., 2007) for 1985–2010 to the Streets et al. (2003) emissions to impose interannual variations in the model. The REAS inventory includes estimated anthropogenic emissions for 1985–2003 based on fuel combustion and industrial sources, as well as projected emissions after 2004 (Jeong and Park, 2013). The long-term simulations of sulfate aerosol concentrations exhibit good agreement with the observations from Acid Deposition Monitoring Network in East Asia (EANET) sites (Jeong and Park, 2013).

2.2. Data

The present study mainly uses the concentration of $PM_{2.5}$ simulated in GEOS-Chem forced by assimilated meteorology from MERRA/NASA. To meet the consistency, therefore, we analyze the atmospheric variables such as precipitation, pressure, and wind are obtained from the MERRA reanalysis data (Rienecker et al., 2011). Focusing on the satellite era from 1979 to the present, MERRA has achieved its goals with significant improvements in precipitation and water vapor climatology (Rienecker et al., 2011). We also analyze the amount of high clouds and low clouds, which are defined by the cloud top pressure from the International Satellite Cloud Climatology Project (ISCCP) (Rossow and Schiffer, 1991). The cloud top pressure of high clouds including deep convection, cirrostratus, and cirrus is 440 hPa to 50 hPa. In contrast, the cloud top pressure of low clouds including the cumulus, stratocumulus, and stratus is 1000 hPa to 680 hPa. The SST dataset is from the global HadISST data from the Met Office Hadley Centre (Rayner et al., 2003). Trends from the SST dataset are removed and the climatological (1986–2010) winter mean is subtracted in order to obtain seasonal anomalies. Unless otherwise stated, results apply to the winter season only (i.e., December to February).

2.3. Idealized model experiments using CAM5

We performed model simulations using the CAM5 model coupled with the Community Land Surface Model version 4 (Neale et al., 2010). The CAM5 model is based on the finite volume (FV) dynamical core at a 1.9° × 2.5° horizontal resolution and with 30 vertical levels. For this study, the ocean and ice modules were not fully coupled, but were communicated to the atmosphere via an oceanic surface boundary condition, given as the mid-month values of SST, as well as sea ice fractions over the polar region. SST and sea ice fractions are time series data constructed by concatenating and interpolating global HadISST data from the Met Office Hadley Centre (Rayner et al., 2003) to the FV core grids of the CAM5. For aerosol simulations, the CAM5 uses a three-mode version of the modal aerosol model (MAM3) (Liu et al., 2012).

To examine the role of pollutant aerosol forcing in East Asia on the precipitation amount in the North Pacific, we updated the Asian anthropogenic SO_2 emissions in the CAM5 with the gridded inventory for 2000 over the Asian domain (60°E–158°E and 13°S–54°N) (Streets et al., 2003). We applied the annual scale factors of REAS (Ohara et al., 2007) for 1985–2010 to the Streets et al. (2003) emissions in order to impose interannual variations in SO_2 emissions in the model. In East Asia, SO_2 emissions continuously increased until 2006 and then slightly decreased. Because the MAM3 module is fully coupled with cloud physics and radiation code, CAM5 accounts for both direct and indirect aerosol effects with the Asian sulfate aerosol change over the recent decades (Neale et al., 2010). We conducted two sets of model experiments using CAM5. The first set, referred to as the SST-run, used the historical SST without East Asian SO_2 emissions. The second set, referred to as the Aerosol-run, included the climatological SST with the time-varying East Asian SO_2 emissions. SO_2 does not fully represent a parameter to examine the pollutant aerosol forcing. In spite of that, SO_2, which is referred to as an evidence of anthropogenic material, is the most dominant pollutant in the atmosphere and it has the highest impact on human origin Ryaboshapko et al., 1983, Charlson et al., 1991, Charlson and Schwartz, 1992, Storelvmo et al., 2016). Each set of experiments was performed with four ensemble members, and the average ensemble mean was presented.

3. Results

Fig. 1a displays the climatological concentration of $PM_{2.5}$ simulated in GEOS-Chem for 1986–2010. Note that the major constituents of $PM_{2.5}$ are anthropogenic aerosols such as sulfate (SO_4^{2-}), nitrate (NO_3^-), ammonium (NH_4^+), black carbon (BC), and organic carbon (OC). A high concentration of climatological concentration of $PM_{2.5}$ is observed in East China. In addition, a structure of climatological concentration of $PM_{2.5}$ extending from the southwest to the northeast in the North Pacific basin is also seen although its concentration is low. We analyze the variability of average $PM_{2.5}$ concentration in East China (110°E–120°E, 28°N–38°N), where the climatological concentration of $PM_{2.5}$ is a maximum (Fig. 1a box). Fig. 1b displays the time series of the averaged $PM_{2.5}$

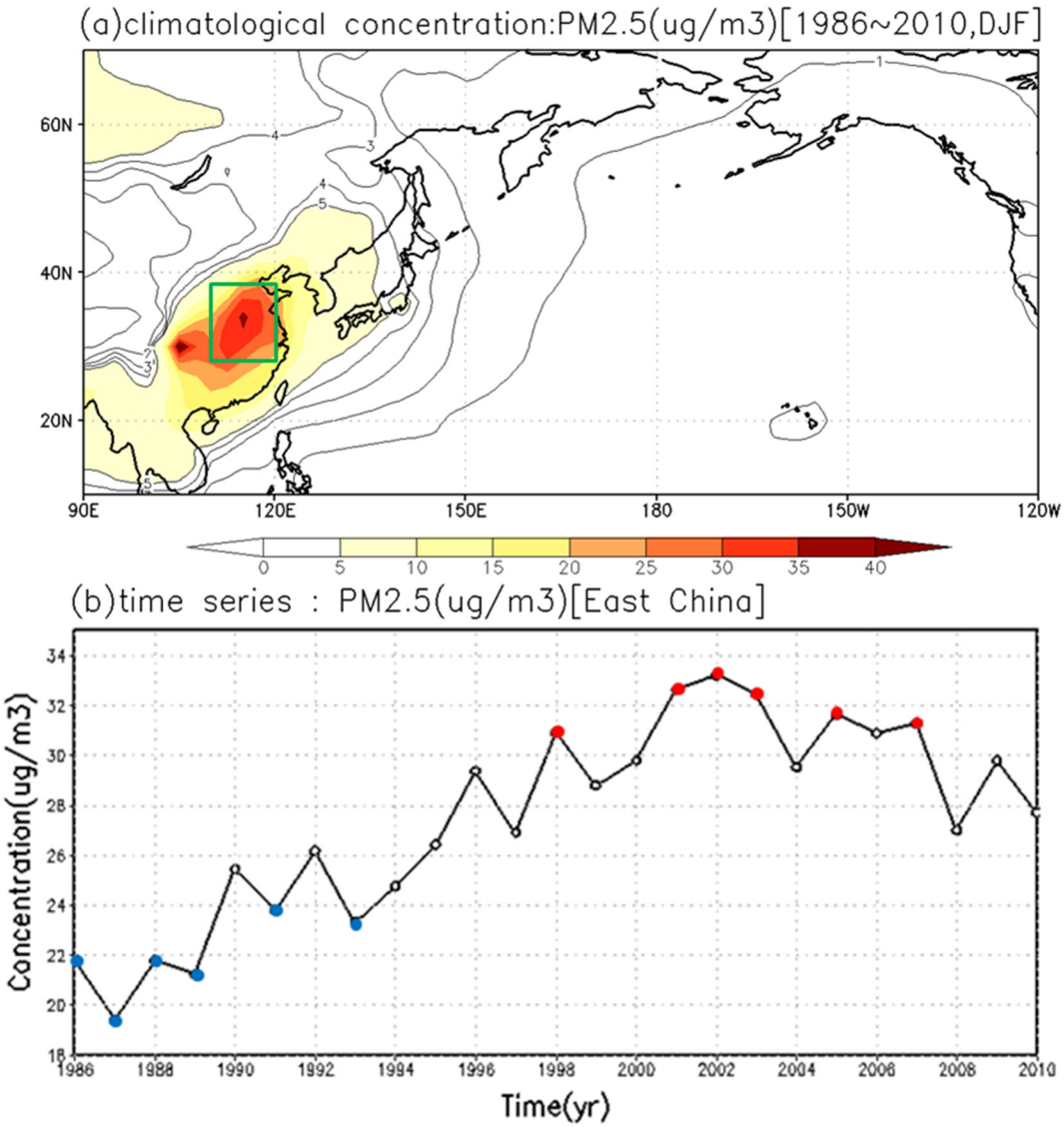

Fig. 1. (a) The spatial pattern of climatological (1986–2010) $PM_{2.5}$ concentration simulated by GEOS-Chem. The box denotes the East China region (28°N–38°N, 110°E–120°E) where the climatological $PM_{2.5}$ concentration is the maximum. (b)The time series of $PM_{2.5}$ averaged in East China for 1986–2010. Red and blue circles in panel b denote the years of high and low $PM_{2.5}$ concentration, respectively.

concentration in East China. Since 1986, the $PM_{2.5}$ concentration gradually increased largely due to rapid Chinese economic development accompanied by increased aerosol emission (Steckel et al., 2015; Lu et al., 2011). However, the $PM_{2.5}$ concentration slightly decreased after the early 2000s, perhaps related to China's policy to reduce aerosol emissions in the recent decade (Zhao et al., 2010; Lei et al., 2011).

To examine the role of $PM_{2.5}$ on precipitation in the North Pacific, we first select the years of high (H-PM period) and low (L-PM period) $PM_{2.5}$ concentration (Table 1). The H-PM period includes the six highest years (1998, 2001, 2002, 2003, 2005, and 2007), while the L-PM period includes the six lowest years (1986, 1987, 1988, 1989, 1991, and 1993) from 1986 to 2010. Note that the winter period includes December to February; for example, the 1986 winter includes December 1985, January 1986, and February 1986. The years of high $PM_{2.5}$ concentration are mostly after the mid-1990s, while the years of low $PM_{2.5}$ concentration are before the mid-1990s. This is largely consistent with Z07 that shows a significant increase in aerosol concentration over the North Pacific after the mid-1990s. Fig. 2 displays the $PM_{2.5}$ concentration during the H-PM and the L-PM periods. It is evident that the $PM_{2.5}$ concentration in East Asia during the H-PM is much higher than during the L-PM period. In addition, the spatial pattern of $PM_{2.5}$ is characterized by a structure extending from East China to the northeast Pacific during both the H-PM and the L-PM periods. In spite of the very low $PM_{2.5}$ concentration, one can see that $PM_{2.5}$ is observed in the North Pacific basin.

Table 1
The years of high and low $PM_{2.5}$ concentration defined by the six highest (1998, 2001, 2002, 2003, 2005, and 2007) and the six lowest (1986, 1987, 1988, 1989, 1991, and 1993) $PM_{2.5}$ concentration years averaged in East China from 1986 to 2010, as shown in Fig. 1b.

$PM_{2.5}$ concentration	Year
High	1998, 2001, 2002, 2003, 2005, 2007
Low	1986, 1987, 1988, 1989, 1991, 1993

Fig. 3a displays the difference of precipitation composite between the H-PM and the L-PM periods (i.e., H-PM period minus L-PM period). First, it is noteworthy that the amount of precipitation increased along the band of climatological precipitation. Specifically, the increase in precipitation amount is prominent in the southwestern part of the climatological precipitation band in the North Pacific. The precipitation increase during the H-PM is evident from the East China Sea to the western North Pacific, where $PM_{2.5}$ is transported from East China by low-level

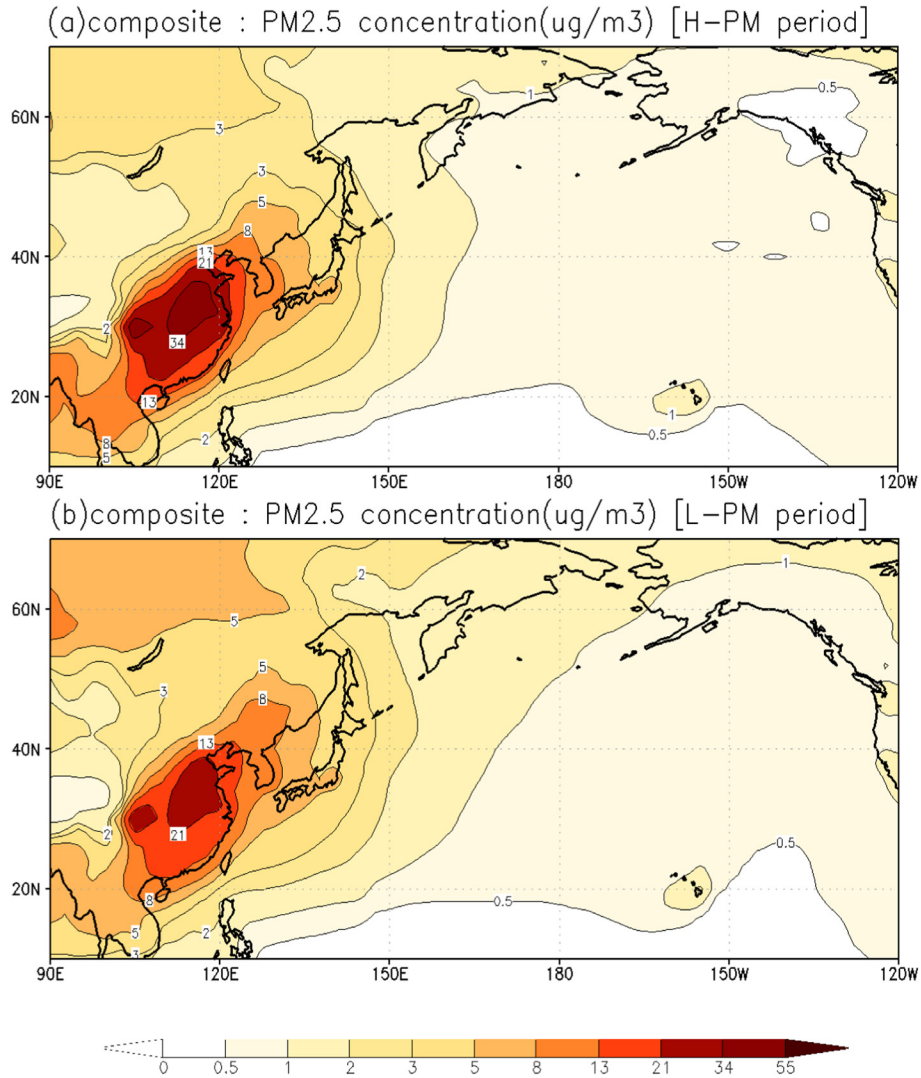

Fig. 2. (a) The composite of $PM_{2.5}$ concentration during the H-PM period and (b) the L-PM period. The unit is μg/m^3.

wind (Fig. 3a). This indicates that the storm track over the North Pacific is shifted slightly to the southwest ward, which might be associated with the increase of $PM_{2.5}$ concentration. Additionally, the precipitation amount is also slightly increased in the central and eastern North Pacific around the west coast of the United States, indicating that the storm track is extended to the east. However, it is not clear whether such precipitation changes in the central and eastern North Pacific are associated with the increase of $PM_{2.5}$ concentration or not.

We also examine the difference in deep convective cloud amounts between the H-PM and the L-PM periods (Fig. 3b). Note that the simultaneous correlation coefficient between the precipitation and the deep convective cloud amount in the North Pacific basin (130°E–120°W, 25°N–50°N) for 1986–2010 is very high at 0.75, which is statistically significant at the 95% confidence level. This indicates that the precipitation in the North Pacific is mostly due to deep convective clouds. The amount of deep convective clouds in the North Pacific basin is also enhanced in the H-PM period where the amount of precipitation is increased (Fig. 3b). In particular, the amount of deep convective clouds is largely increased in the eastern North Pacific, indicating that the storm track is extended to the east in the North Pacific during the H-PM period, which is consistent with the precipitation changes shown in Fig. 3a.

In addition, the amount of deep convective clouds is also enhanced in the southwestern part of North Pacific. This indicates that such an enhancement might be associated with the increase in $PM_{2.5}$ concentration originated from East China, leading to changes in precipitation amount as well as the storm track. This effect mostly occurred after the mid-1990s when the $PM_{2.5}$ concentration was high in East China (i.e., H-PM period). These results are consistent to some extent with Z07's argument that an increase in deep convective clouds, as well as the intensification of storm track, over the North Pacific Ocean in winter since the mid-1990s is mainly due to the aerosol effect from the Asian pollution outflow.

In spite of this, however, we cannot exclude the possibility that the increase in precipitation amount in the North Pacific from the H-PM to the L-PM (Fig. 3a) is associated with the SST forcings in the tropical Pacific. To examine this, we first display the difference in SST composite between the H-PM and the L-PM periods (Fig. 4). We find that the SST in the central-to-eastern tropical Pacific is warmer in the H-PM than in the L-PM. It is found that the El Niño-like warming may contribute to increase the PM_2.5 concentration in East China (Fig. 5). That is, El Niño-like SST warming in the central tropical Pacific forces the atmospheric circulations (Jeing and Park, 2017, Yim et al., 2008, Wang, 2001, Wang et al., 2000), leading to the low-level (850 hPa) convergence in East China. This contributes to increase the PM_2.5 concentration as shown in Fig. 5. In addition, El Niño-like SST warming is associated with a weakening of East Asian winter monsoon (see Fig.

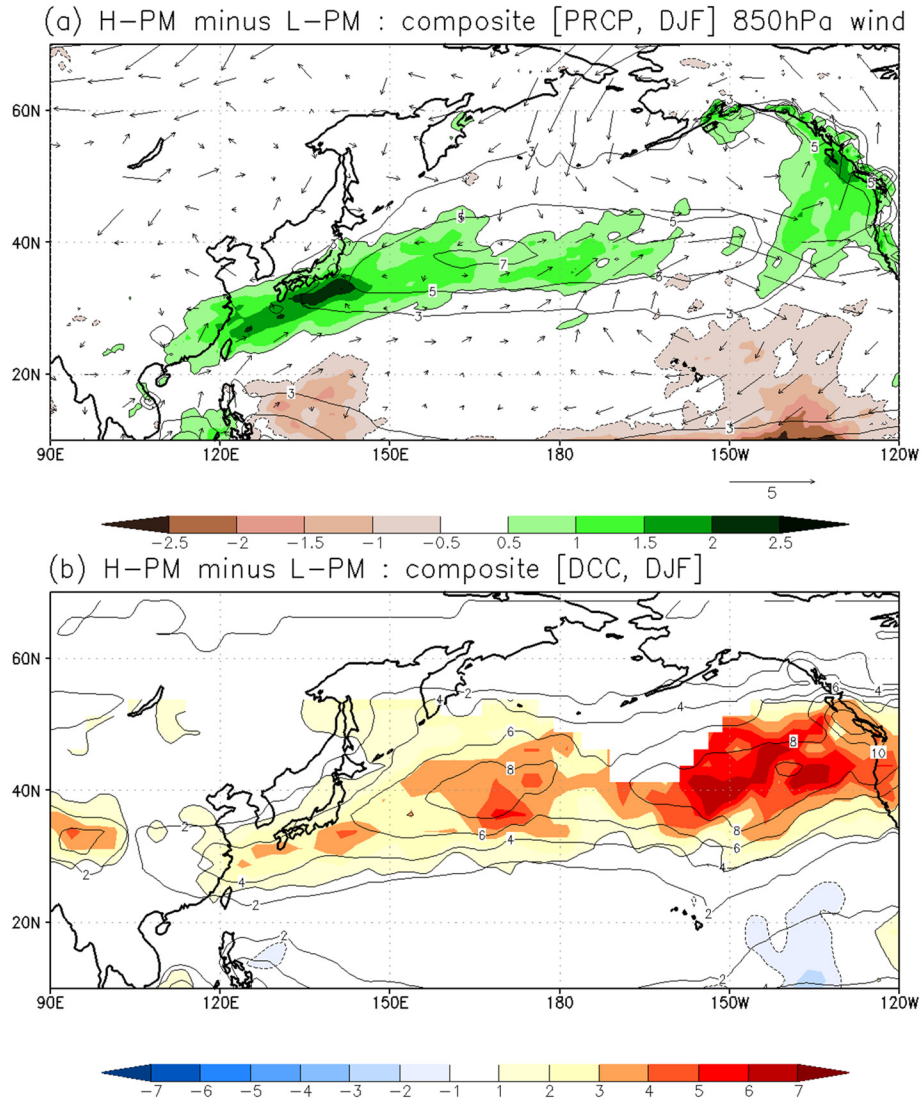

Fig. 3. (a) Precipitation and 850 hPa wind difference between the H-PM and the L-PM period (H-PM period minus L-PM period) (precipitation is shading and 850 hPa wind is vector). Contour lines are the climatological precipitation amount. The unit is mm/day. (b) Deep convective cloud amount difference between the H-PM and the L-PM period (shading). Contour lines are the climatological amount of deep convective cloud and unit is %.

3a), which is associated with a weakening of wind speed. This also results in the increase of PM2.5 concentration (Jeing and Park, 2017).

On the other hand, there is a possibility that the El Niño-like warming may influence the precipitation amount in the North Pacific in the H-PM period compared to the L-PM period. According to previous studies, El Niño-related precipitation anomalies over the Pacific are related to storm track changes in the North Pacific (Seager et al., 2010). It is known that the storm track is displaced further to the south and also extended to the east over the eastern Pacific during El Niño events (Hoerling and Ting, 1994; Trenberth and Hurrell, 1994; Chang, 2006; Eichler and Higgins, 2006; Seager et al., 2010). This is somewhat consistent with our results based on the difference in precipitation and deep convective cloud amounts between the H-PM and the L-PM periods (Fig. 3). Therefore, the role of El Niño-like warming in the H-PM period should be considered when analyzing the role of pollutant aerosols on the precipitation amount in the North Pacific.

To examine the relative contribution of $PM_{2.5}$ and SST forcing on precipitation variability in the North Pacific, we analyze two model experiments for 1986–2010 (i.e., SST-run and Aerosol-run). The SST-run is forced by the historical SST without the East Asian SO_2 emissions. In contrast, the Aerosol-run is forced by the climatological SST with the time-varying East Asian SO_2 emissions. Therefore, there are no emission changes in the SST-run in order to exclude the role of sulfate aerosol pollutants. In contrast, the climatological SST is prescribed in the Aerosol-run to exclude the influence of SST forcing. Although only SO_2 is considered among the $PM_{2.5}$ particles in the Aerosol-run, the comparison between the SST-run and the Aerosol-run may indicate the relative roles of Asian pollutant aerosol and SST forcings on precipitation variability in the North Pacific. Note the climatological (1986–2010) composition of $PM_{2.5}$ simulated in the GEOS-Chem in East China during winter is 30% SO_4^{2-}, 30% NO_3^-, 19% NH_4^+, 7% BC, and 14% OC.

Fig. 6 displays the difference in precipitation and wind at 850 hPa composite between the H-PM and the L-PM periods (H-PM period minus L-PM period) in the SST-run and the Aerosol-run, respectively. Note that the difference in SST composite between the H-PM and the L-PM in the SST-run is the same as that shown in Fig. 4. Therefore, Fig. 6a displays the response of precipitation and 850 hPa wind due to the El Niño-like warming in the SST-run, not the Asian pollutant aerosol forcing. In the SST-run, the precipitation amount increased in the central and eastern North Pacific where the anomalous atmospheric circulation is largely influenced by the atmospheric teleconnection due to the El Nino-like warming (Wallace and Gutzler, 1981). In particular, the

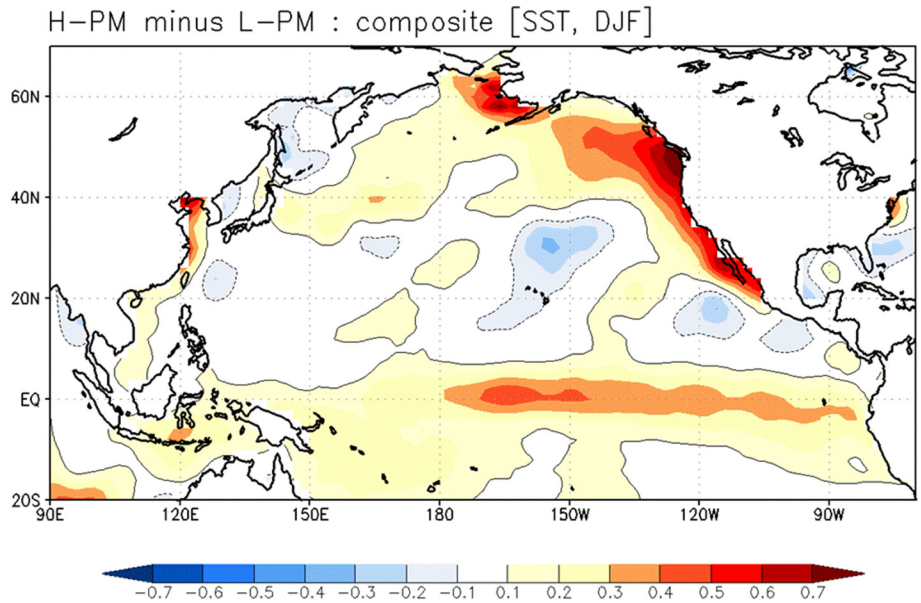

Fig. 4. SST difference between the H-PM and L-PM periods (H-PM period minus L-PM period). The unit is °C.

maximum of the increased precipitation is located in the eastern North Pacific around the west coast of the United States (Fig. 6a), which is largely due to a strengthening of Aleutian low pressure in relation to the El Niño-like warming (Alexander et al., 2002). This indicates that the storm track over the North Pacific is extended to the east over the eastern North Pacific, which is largely consistent with previous studies. Therefore, the precipitation change due to the El Niño-like warming in the SST-run (Fig. 5a) partly explains the observation between the H-PM and the L-PM period in the central-to-eastern North Pacific as shown in Fig. 3a.

On the other hand, the precipitation change in the Aerosol-run is limited in the East Asia marginal sea and the central Pacific (Fig. 6b), which is a bit similar to the observation as shown in Fig. 3a. However, there also exist some discrepancies. The increase of precipitation amount during the H-PM period is small in the Aerosol-run, in addition, the region where the precipitation amount increases is shifted to the south in the southwestern North Pacific compared to the observation. The maximum increase of precipitation amount is located in the south of Japan in the observation (Fig. 3). Such discrepancies might be due to several reasons including the model deficiency simulating the precipitation or the Aerosol-run is only considering the sulfate aerosol among the $PM_{2.5}$. For example, the concentration of nitrate, which is not considered in the Aerosol-run, is also quite high during boreal winter (Zhao et al., 2010). It is noteworthy that the Aerosol-run fails to simulate the increase of precipitation amount in the central and eastern North Pacific, which is unlike the SST-run. Therefore, these results indicate that both the SST forcing and the Asian pollutant particles contribute to changes in precipitation amount and storm track intensity in the

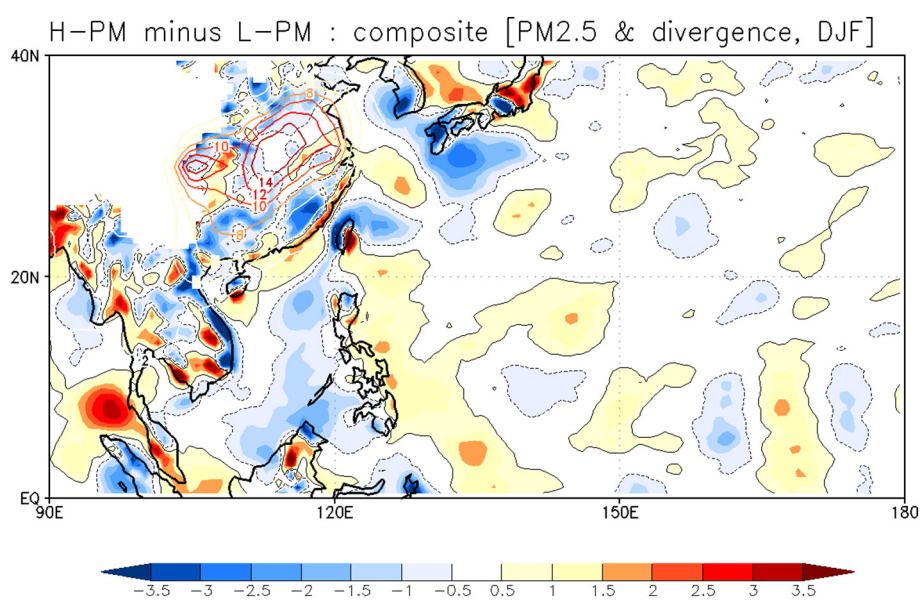

Fig. 5. The difference of PM2.5 concentration (contour) and 850 hPa divergence (shading) between the H-PM and the L-PM period (H-PM period minus L-PM period). The contour is PM2.5 concentration (unit is $\mu g/m^3$) and the shading denotes a 850 hPa divergence (unit is $10^{-6}\ s^{-1}$).

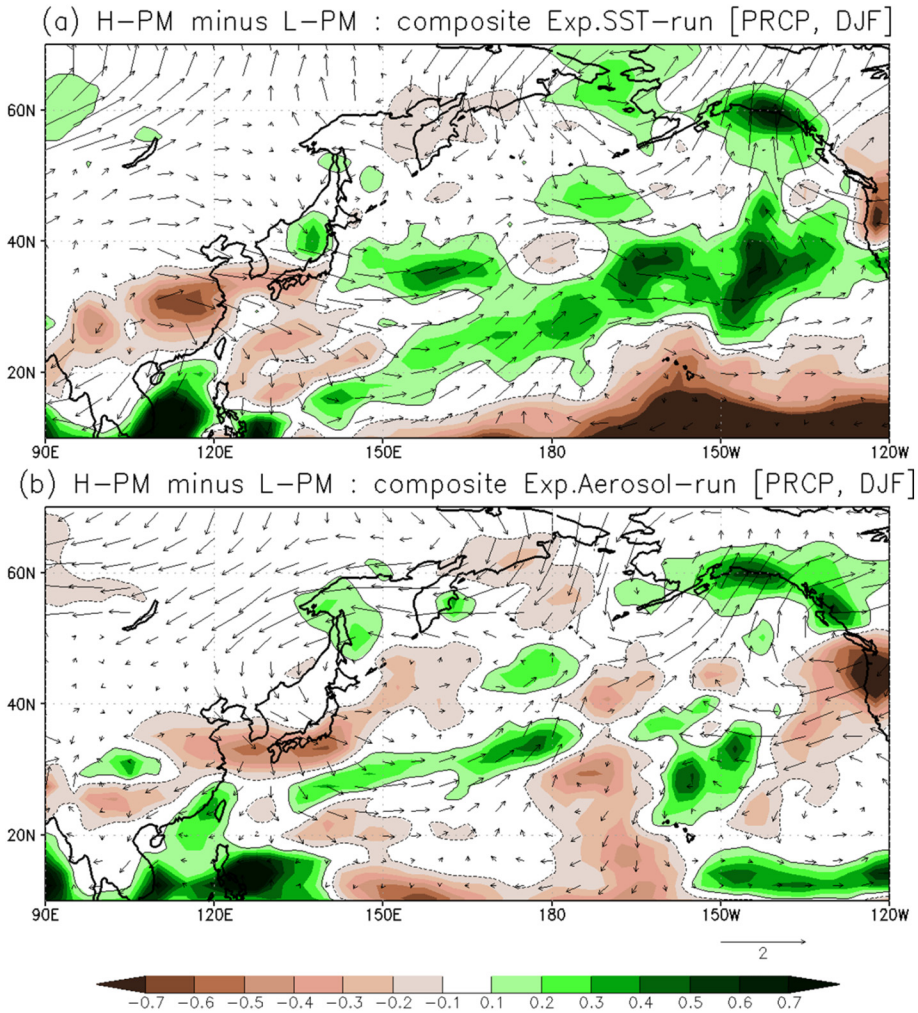

Fig. 6. (a) Precipitation and 850 hPa wind difference between the H-PM and the L-PM periods in the SST-run and (b) the Aerosol-run. Contour lines are the climatological mean precipitation. Unit is mm/day.

North Pacific. In particular, the SST forcing more contributes to change in the precipitation amount in the central and eastern North Pacific, which is in contrast to the role of Aerosol pollutant particles whose influences are dominant in the southwestern Pacific.

4. Summary

To understand the relative roles of Asian pollutant aerosols and SST forcings on precipitation in the North Pacific, we analyzed the interannual variation of $PM_{2.5}$ and model experiments. The $PM_{2.5}$ concentration is obtained from GEOS-Chem using the assimilated meteorology from the MERRA for 1985–2010. The average concentration of $PM_{2.5}$ in East China gradually increased since 1986, then slightly decreased after the early 2000s. Using the time series of $PM_{2.5}$ concentration, years of high and low $PM_{2.5}$ concentration of $PM_{2.5}$ are defined as the H-PM period and the L-PM period, respectively. The composite analysis between the two periods indicated that changes in the deep convective cloud amount, as well as the precipitation amount, in the North Pacific might be associated with increases in $PM_{2.5}$ concentration. However, an El Niño-like warming was evident in the H-PM period indicating the possibility that the El Niño-like warming may influence the precipitation amount in the North Pacific in the H-PM compared to the L-PM period.

To examine the relative contribution of Asian pollutant aerosols and SST forcing on precipitation amounts in the North Pacific, two idealized experiments (i.e., SST-run and Aerosol-run) were analyzed. The SST-run used the historical SST without East Asian SO_2 emissions and the Aerosol-run included the climatological SST with the time-varying East Asian SO_2 emissions. By comparing with the precipitation simulated in these two experiments, we understood the relative roles of Asian pollutant aerosols and SST forcings on precipitation change in the North Pacific. We found that the precipitation amount increased in the central and eastern North Pacific, along with a maximum of increased precipitation in the eastern North Pacific around the west coast of United States, in the SST-run. This indicated that the storm track over the Pacific was extended to the east over the eastern North Pacific, and that the precipitation change due to the El Niño-like warming in the SST-run should be considered to explain the observed changes in the precipitation amount in the H-PM period. On the other hand, the increase in precipitation in the western and central North Pacific observed in the H-PM period was simulated to some extent in the Aerosol-run although there exist some discrepancies. Therefore, both the SST forcing and the Asian pollutant particles contribute to changes in the amount of precipitation, as well as the intensity of the storm track, in the North Pacific. This implies that it is important to consider both the SST forcing and the Asian pollutants to understand precipitation variability and storm track intensity in the North Pacific. However, the Aerosol-run model experiments conducted in the present study were done by the time-varying East Asian SO_2 emissions, which is limited to fully understand the role of Asian pollutions. Therefore, it is necessary to conduct model experiments which simulate the whole representative parameters to examine the pollutant aerosol forcings in East Asia.

Acknowledgement

This study was supported by the Korea Ministry of Environment (MOE) as "Climate Change Correspondence Program."

References

Ackerman, A.S., Toon, O., Stevens, D., Heymsfield, A., Ramanathan, V., Welton, E., 2000. Reduction of tropical cloudiness by soot. Science 288, 1042–1047.
Albrecht, B.A., 1989. Aerosols, cloud microphysics, and fractional cloudiness. Science 245, 1227–1230.
Alexander, M.A., Blade, I., Newman, M., Lanzante, J.R., Lau, N.C., Scott, J.D., 2002. The atmospheric bridge: the influence of ENSO teleconnections on air-sea interaction over the global oceans. J. Clim. 15 (16), 2205–2231.
Allen, M.R., Fuglestvedt, J.S., Shine, K.P., Reisinger, A., Pierrehumbert, R.T., Forster, P.M., 2016. New use of global warming potentials to compare cumulative and short-lived climate pollutants. Nat. Clim. Chang. 6:773–776. http://dx.doi.org/10.1038/nclimate2998.
Boo, K.O., Booth, B.B., Byun, Y.H., Lee, J., Cho, C., Shim, S., Kim, K.T., 2015. Influence of aerosols in multidecadal SST variability simulations over the North Pacific. J. Geophys. Res. 120, 517–531.
Chang, E.K., 2006. An idealized nonlinear model of the Northern Hemisphere winter storm tracks. J. Atmos. Sci. 63, 1818–1839.
Chang, E.K., Lee, S., Swanson, K.L., 2002. Storm track dynamics. J. Clim. 15, 2163–2182.
Charlson, R.J., Langner, J., Rodhe, H., Leovy, C., Warren, S., 1991. Perturbation of the northern hemisphere radiative balance by backscattering from anthropogenic sulfate aerosols. Tellus A 43, 152–163.
Charlson, R.J., Schwartz, S., 1992. Climate forcing by anthropogenic aerosols. Science 255, 423.
Chung, C.E., Ramanathan, V., Kiehl, J.T., 2002. Effects of the South Asian absorbing haze on the northeast monsoon and surface-air heat exchange. J. Clim. 15, 2462–2476.
Eichler, T., Higgins, W., 2006. Climatology and ENSO-related variability of North American extratropical cyclone activity. J. Clim. 19, 2076–2093.
Elliott, S., Shen, M., Blake, D.R., Lu, R., Russell, A.G., Kao, C., Streit, G.E., Zhao, X.P., McCREARY, E.I., Rowland, F.S., 1997. Atmospheric effects of the emerging mainland Chinese transportation system at and beyond the regional scale. J. Atmos. Chem. 27, 31–70.
Fan, J., Yuan, T., Comstock, J.M., Ghan, S., Khain, A., Leung, L.R., Li, Z., Martins, V.J., Ovchinnikov, M., 2009. Dominant role by vertical wind shear in regulating aerosol effects on deep convective clouds. J. Geophys. Res. 114. http://dx.doi.org/10.1029/2009JD012352.
Haywood, J., Boucher, O., 2000. Estimates of the direct and indirect radiative forcing due to tropospheric aerosols: a review. Rev. Geophys. 38, 513–543.
Hoerling, M.P., Ting, M., 1994. Organization of extratropical transients during El Nino. J. Clim. 7, 745–766.
Jeing, J.I., Park, R.J., 2017. Winter monsoon variability and its impact on aerosol concentrations in East Asia. Environ. Pollut. 221, 285–292.
Jeong, J.I., Park, R.J., 2013. Effects of the meteorological variability on regional air quality in East Asia. Atmos. Environ. 69, 46–55.
Jiang, H., Feingold, G., 2006. Effect of aerosol on warm convective clouds: aerosol-cloud-surface flux feedbacks in a new coupled large eddy model. J. Geophys. Res. 111. http://dx.doi.org/10.1029/2005JD006138.
Kim, M.-J., Yeh, S.-W., Park, R.J., 2016. Effect of sulfate aerosol on East Asian summer monsoon. Geophy. Res. Letts. 43. http://dx.doi.org/10.1002/2015GL067124.
Lau, N.-C., Nath, M.J., 1996. The role of the "atmospheric bridge" in linking tropical Pacific ENSO events to extratropical SST anomalies. J. Clim. 9, 2036–2057.
Lee, S.-Y., Shin, H.-J., Wang, C., 2013. Nonlinear effects of coexisting surface and atmospheric forcing of anthropogenic absorbing aerosols: impact on the South Asian monsoon onset. J. Clim. 26, 5594–5607.
Lei, Y., Zhang, Q., He, K., Streets, D., 2011. Primary anthropogenic aerosol emission trends for China, 1990–2005. Atmos. Chem. Phys. 11, 931–954.
Liu, X., Easter, R.C., Ghan, S.J., Zaveri, R., Rasch, P., Shi, X., Lamarque, J.-F., Gettelman, A., Morrison, H., Vitt, F., 2012. Toward a minimal representation of aerosols in climate models: description and evaluation in the Community Atmosphere Model CAM5. Geosci. Model Dev. 5, 709.
Lu, Z., Zhang, Q., Streets, D.G., 2011. Sulfur dioxide and primary carbonaceous aerosol emissions in China and India, 1996–2010. Atmos. Chem. Phys. 11, 9839–9864.
Meehl, G.A., Arblaster, J.M., Collins, W.D., 2008. Effects of black carbon aerosols on the Indian monsoon. J. Clim. 21, 2869–2882.
Neale, R.B., Chen, C.-C., Gettelman, A., Lauritzen, P.H., Park, S., Williamson, D.L., Conley, A.J., Garcia, R., Kinnison, D., Lamarque, J.-F., 2010. Description of the NCAR community atmosphere model (CAM 5.0). NCAR Tech. Note NCAR/TN-486 + STR, p. 274.
Ohara, T., Akimoto, H., Kurokawa, J.-I., Horii, N., Yamaji, K., Yan, X., Hayasaka, T., 2007. An Asian emission inventory of anthropogenic emission sources for the period 1980–2020. Atmos. Chem. Phys. 7, 4419–4444.
Park, R.J., Jacob, D.J., Field, B.D., Yantosca, R.M., Chin, M., 2004. Natural and transboundary pollution influences on sulfate-nitrate-ammonium aerosols in the United States: implications for policy. J. Geophys. Res. 109. http://dx.doi.org/10.1029/2003JD004473.
Rayner, N., Parker, D.E., Horton, E., Folland, C., Alexander, L., Rowell, D., Kent, E., Kaplan, A., 2003. Global analyses of sea surface temperature, sea ice, and night marine air temperature since the late nineteenth century. J. Geophys. Res. 108. http://dx.doi.org/10.1029/2002JD002670.
Rienecker, M.M. and Coauthors, 2011. MERRA: NASA's modern-era retrospective analysis for research and applications. J. Clim. 24, 3624–3648.
Rossow, W.B., Schiffer, R.A., 1991. ISCCP cloud data products. Bull. Am. Meteorol. Soc. 72, 2–20.
Ryaboshapko, A., Ivanov, M.V., Freney, J.R., 1983. The Atmospheric Sulfur Cycle, the Global Biogeochemical Sulfur Cycle (SCOPE Report 19), 203–296. John Wiley, New York.
Seager, R., Naik, N., Ting, M., Cane, M., Harnik, N., Kushnir, Y., 2010. Adjustment of the atmospheric circulation to tropical Pacific SST anomalies: variability of transient eddy propagation in the Pacific–North America sector. Q. J. R. Meteorol. Soc. 136, 277–296.
Steckel, J.C., Edenhofer, O., Jakob, M., 2015. Drivers for the renaissance of coal. PNAS 112, E3775–E3781.
Stevens, B., Feingold, G., 2009. Untangling aerosol effects on clouds and precipitation in a buffered system. Nature 461, 607–613.
Stocker, T.F., et al., 2013. Technical Summary. In: Stocker, T.F., Qin, D., Plattner, G.-K., Tignor, M., Allen, S.K., Boschung, J., Nauels, A., Xia, Y., Bex, V., Midgley, P.M. (Eds.), Climate Change 2013: The Physical Science Basis. Contribution of Working Group I to the Fifth Assessment Report of the Intergovernmental Panel on Climate Change. Cambridge University Press, Cambridge, United Kingdom and New York, NY, USA.
Storelvmo, T., Leirvik, T., Lohmann, U., Phillips, P.C.B., Wild, M., 2016. Disentangling greenhouse warming and aerosol cooling to reveal Earth's climate sensitivity. Nat. Geosci. 9, 286–291.
Streets, D.G., Bond, T., Carmichael, G., Fernandes, S., Fu, Q., He, D., Klimont, Z., Nelson, S., Tsai, N., Wang, M.Q., 2003. An inventory of gaseous and primary aerosol emissions in Asia in the year 2000. J. Geophys. Res. 108. http://dx.doi.org/10.1029/2002JD003093.
Tao, W.K., Chen, J.P., Li, Z., Wang, C., Zhang, C., 2012. Impact of aerosols on convective clouds and precipitation. Rev. Geophys. 50. http://dx.doi.org/10.1029/2011RG000369.
Trenberth, K.E., Hurrell, J.W., 1994. Decadal atmosphere-ocean variations in the Pacific. Clim. Dyn. 9, 303–319.
Twomey, S., 1974. Pollution and the planetary albedo. Atmos. Environ. 8, 1251–1256.
Twomey, S., 1977. The influence of pollution on the shortwave albedo of clouds. J. Atmos. Sci. 34, 1149–1152.
Van Aardeen, G.C., Streets, D., Levy, H., Hordijk, L., 1998. NOx emissions in Asia from Anthropogenic Activities. Atmos. Environ. 33, 633–646.
Wallace, J.M., Gutzler, D.S., 1981. Teleconnections in the geopotential height field during the Northern Hemisphere winter. Mon. Weather Rev. 109, 784–812.
Wang, C., 2001. Atmospheric circulation cells associated with the El Nino Southern Oscillation. J. Clim. 15, 399–419.
Wang, C., 2013. Impact of anthropogenic absorbing aerosols on clouds and precipitation: a review of recent progresses. Atmos. Res. 122, 237–249.
Wang, B., Fu, X., Wu, R., 2000. Pacific-East Asian teleconnection: how does ENSO affect East Asian climate? J. Clim. 13, 1517–1536.
Wang, Y., Zhang, R., Saravanan, R., 2014. Asian pollution climatically modulates mid-latitude cyclones following hierarchical modelling and observational analysis. Nat. Commun. 5. http://dx.doi.org/10.1038/ncomms4098.
Yeh, S.-W., Kim, W.M., Kim, Y.H., Moon, B.K., Park, R.J., Song, C.K., 2013. Changes in the variability of the North Pacific sea surface temperature caused by direct sulfate aerosol forcing in China in a coupled general circulation model. J. Geophys. Res. 118, 1261–1270.
Yeh, S.-W., Park, R.J., Kim, M., Jeong, J., Song, C.-K., 2015. Effect of anthropogenic sulphate aerosol in China on the drought in the western-to-central US. Sci. Rep. 5:14305. http://dx.doi.org/10.1038/srep14305.
Yim, S.-Y., Jhun, J.-G., Yeh, S.-W., 2008. Decadal change in the relationship between east Asian/western North Pacific summer monsoon system and ENSO around the mid-1990s. Geophys. Res. Lett. 35, L20711. http://dx.doi.org/10.1029/2008GL035751.
You, Q.L., et al., 2011. Changes in daily climate extremes in China and their connection to the large scale atmospheric circulation during 1961–2003. Clim. Dyn. 36, 2399–2417.
Zhang, R., Li, G., Fan, J., Wu, D.L., Molina, M.J., 2007. Intensification of Pacific storm track linked to Asian pollution. Proc. Natl. Acad. Sci. 104, 5295–5299.
Zhao, Y., Wang, S., Nielsen, C.P., Li, X., Hao, J., 2010. Establishment of a database of emission factors for atmospheric pollutants from Chinese coal-fired power plants. Atmos. Environ. 44, 1515–1523.
Zhou, T., Yu, R., Chen, H., Dai, A., Pan, Y., 2008. Summer precipitation frequency, intensity, and diurnal cycle over China: a comparison of satellite data with rain gauge observations. J. Clim. 21 (16), 3997–4010.